GEOMETRICAL STUDY OF MIDDLE KINGDOM FUNERARY COMPLEXES IN QUBBET EL-HAWA (ASWAN, EGYPT) BASED ON 3D MODELS

ESTUDIO GEOMÉTRICO DE COMPLEJOS FUNERARIOS DEL REINO MEDIO EN QUBBET EL-HAWA (ASUÁN, EGIPTO) BASADO EN MODELOS 3D

Antonio Tomás Mozas-Calvache* , José Luis Pérez-García , José Miguel Gómez-López

a Department of Cartographic Engineering, Geodesy and Photogrammetry, University of Jaén, Campus Las Lagunillas, 23071 Jaén, Spain. antmozas@ujaen.es; jlperez@ujaen.es; jglopez@ujaen.es

Highlights:

- A new methodology is presented to develop geometrical analysis of burial structures based on 3D models.

- The methodology has been applied to three contiguous burial structures (hypogea), allowing the researchers to analyse some constructive aspects such as dimensions, proportions, orientations, flatness and inclinations.

- Results have demonstrated the advanced skills achieved by ancient Egyptians in construction techniques.

Abstract:

This study describes the methodology developed and the main results obtained when analysing the geometrical behaviour of three adjacent burial structures located in southern Egypt. The rock-cut tombs are composed of complex geometries such as halls, corridors, chambers and vertical shafts. Among other determining aspects, this complexity greatly conditioned the data acquisition and processing work. In this context, the main objective of this study was to develop a new methodology for obtaining geomatic products that support a complete geometrical analysis of the tombs. The researchers have used photogrammetric and laser scanning surveys to obtain accurate 3D models on a common reference system. The procedure used included obtaining several secondary products, such as several geometries (planes and cylinders) fitted from point clouds or plans and sections obtained from the 3D models. The geometric analysis has included several aspects: dimensions, proportions, orientations, wall flatness, inclinations, etc., and it is based on these products. The results obtained suggest and confirm several hypotheses about the constructive aspects of these hypogea based on a large amount of data, including the determination of a proportional canon used by the ancient Egyptians to plan and perform the excavation works of each funerary structure. The application of this methodology has demonstrated that this type of analysis is viable to unveil some important aspects of these structures and the constructive procedures carried out almost four millennia ago.

Keywords: archaeology; burial structures; 3D model; photogrammetry; terrestrial laser scanning

Resumen:

Este estudio describe la metodología desarrollada y los principales resultados obtenidos al analizar el comportamiento geométrico de tres estructuras funerarias contiguas situadas en el sur de Egipto. Las tumbas excavadas en la roca están compuestas de estructuras complejas como salas, pasillos, cámaras y pozos. Entre otros aspectos, esta complejidad condicionaba en gran medida la adquisición de datos y el trabajo de procesado. En este contexto, el objetivo principal de este estudio fue desarrollar una nueva metodología para obtener productos geomáticos que facilitaran un análisis geométrico completo de las tumbas. Se han realizado diversos levantamientos fotogramétricos y de escaneado láser terrestre para obtener modelos 3D de precisión en un mismo sistema de referencia. El procedimiento utilizado incluyó la obtención de varios productos secundarios, como varias geometrías (planos y cilindros) ajustadas desde las nubes de puntos, o planos y secciones obtenidas de los modelos 3D. El análisis geométrico ha incluido distintos aspectos de la geometría: dimensiones, proporciones, orientaciones, planeidad de muros, inclinaciones, etc., y está basado en estos productos. Los resultados obtenidos sugieren y confirman ciertas hipótesis acerca de los aspectos constructivos de estos hipogeos basados en una gran cantidad de datos, incluyendo la determinación de un canon proporcional utilizado por los antiguos egipcios para planificar y ejecutar los trabajos de excavación de cada estructura funeraria. La aplicación de esta metodología ha demostrado que este tipo de análisis es viable para detectar algunos aspectos importantes de estas estructuras y de los procedimientos constructivos llevados a cabo hace casi cuatro milenios.

Palabras clave: arqueología; estructuras funerarias; modelo 3D; fotogrametría; láser escáner terrestre

---

* Corresponding author: Antonio Tomás Mozas-Calvache, antmozas@ujaen.es

1. Introduction

The current availability of geomatic techniques allows fast and accurate three-dimensional (3D) documentation of archaeological sites, even of complex scenes, by providing 3D models of their structures. Among other cases, this is especially important in rock-cut burial complexes such as Egyptian hypogea, where the presence of narrow spaces, vertical shafts and other complicated conditions is usual. The application of recent methodologies based on close-range photogrammetry (CRP) and light detection and ranging (LiDAR), and more specifically on terrestrial laser scanning (TLS), allows the obtaining of 3D models to document these structures determining their geometry with a density and accuracy unimaginable until recent years. Other aspects, such as the efficiency of data acquisition or processing, have become essential in the development of these studies of documentation, if we consider the impossibility, or at the very least, the great workload implied in the application of traditional techniques. In addition to documentation purposes, features of these products provide the opportunity to develop geometrical and structural analyses of these funerary complexes in order to study their construction procedures.

1.1. Geomatics techniques applied to archaeological sites

In this context, the great expansion of CRP applications in archaeological sites is based on three main aspects: Firstly, the common use of low-cost non-metric cameras (Ogleby et al., 1999; Celikoyan, 2003; Cardenal et al., 2004; Chandler et al., 2005; Covas et al., 2015; Fiorillo et al., 2016; Barazzetti, 2017a and 2017b). Secondly, the improvement of techniques for acquiring photographs (Waldhäusl & Ogleby, 1994), using different platforms to lift cameras such as masts (Georgopoulos, 2003; Mozas-Calvache et al. 2012; Martínez et al. 2013; Ortiz et al., 2013; Blockley & Morandi, 2015; Pérez et al., 2018) or remotely piloted aircraft systems (RPAS) (Colomina & Molina, 2014; Nex & Remondino, 2014; Campana, 2017). Thirdly, the development of processing algorithms such as structure from motion (SfM) (Ullman, 1979; Koenderink & Van Doorn, 1991; Lowe, 2004; Szeliski, 2011) and the dense multiview stereo 3D reconstruction (MVS) (Scharstein & Szeliski, 2002; Seitz et al., 2006; Szeliski, 2011; Furukawa & Hernández, 2015) and their implementation in widely-distributed software packages (Brutto & Meli, 2012). All these aspects have allowed a 'democratization' of photogrammetry, opening its use to non-professional users (Westoby et al., 2012). In addition to these improvements in methods and techniques, the final products demanded in these types of studies have also undergone a significant change, from simple plans (obtained by plotting) to the generation of 3D models, orthoimages and digital elevation models (DEM). To summarise, we can indicate that all these aspects have supposed a revolution in the field of photogrammetry applied to archaeological sites and heritage.

On the other hand, the development and improvement of active sensors to document heritage, such as laser scanning devices (Beraldin et al., 2000), has also undergone a remarkable evolution in recent times. Thus, the application of LiDAR techniques, and more specifically of TLS, to archaeological sites has undergone a great expansion due to improvements in efficiency and accuracy, but also the progressive reduction of cost with respect to devices available years ago. In general, the main product demanded in these applications for 3D documentation of the object (terrain or artefacts) is 3D models.

The selection of the technique to be used (including the integration of both) will depend on the scene under study, the availability of instruments and other circumstances such as the budget of the project, location constraints, the time needed for acquisition, goal of the model, illumination conditions, permissions, etc. (Lambers & Remondino, 2007; Mozas-Calvache et al., 2020). However, both techniques, CRP and TLS, are compatible, and their use must not be considered independently. Thus, several studies have demonstrated the benefits of the integration of the two (Kadobayashi et al., 2004; Ahmon, 2004; Alshawabkeh & Haala, 2004; Guarnieri et al., 2006; Grussenmeyer et al., 2008; Nabil et al., 2013; Lima & Vergauwen, 2018) because of the global improvement achieved when considering particular advantages of each technique. In this sense, some authors, such as Hassani et al. (2015), have described the advantages and disadvantages of applying CRP and TLS. Thus, although both techniques allow us to obtain 3D models, CRP provides more realistic textures and usually supposes the best option for generating other products (e.g. orthoimages), while TLS allows for the fast acquisition of dense point clouds. The use of CRP supposes an alternative in cases where a low-cost technique must be considered, or a high-quality realistic texture of the structure is demanded (e.g. VR applications). However, the difficulties involved in the acquisition of photographs in these structures make it contingent on the use of this technique because of the necessity to cover the entire object from several points of view while guaranteeing homogeneous illumination conditions. In this sense, the presence of narrow spaces could increase the number of photographs needed to cover the structure using normal focal lenses mounted in non-metric cameras. The use of TLS supposes a viable option in these scenes. In the case of complex sites, TLS supposes an excellent and powerful method for collecting 3D data and creating accurate surface models (Remondino et al., 2011). The establishment of several scanning stations can encounter difficulties caused by warped structures. The acquisition time is also relatively low at each station and more effective if the capture does not consider the acquisition of high dynamic range (HDR) images. This will suppose the combination with CRP if the requirements include real textures. In addition, the illumination conditions do not affect scans without colour acquisition. Even in complex spaces and structures, TLS has shown great results as demonstrated by Colonnese et al. (2016) and Mozas-Calvache et al. (2020). The presence of narrow spaces suggests the addition of more scanning stations to cover the structure completely in spite of the low increment of time caused by each scan. New techniques based on handheld laser scanning (e.g. Geoslam ZEB Go, Leica BLKGO, etc.) can be used to improve the efficiency of data acquisition, although the accuracy is currently lower than stop-and-go scanners. Some interesting studies of complex scenarios using these mobile techniques have been described in this context, such as Zlot & Bosse (2014) and Farella (2016).

In the case of complex scenes such as hypogea, some examples of the application of these techniques (independently or combined) have recently been

described in the literature. Some examples of applications based on CRP are Angelini et al. (2016) and Pérez-García et al. (2019). In the case of TLS, we highlight studies such as Ahmon (2004), Nabil et al. (2013), Lima & Vergauwen (2018) and Echeverría et al. (2019). In general, the main issue with these types of studies is related to the presence of reduced and narrow spaces which makes the application highly contingent on the methodology to be used. In this sense, several studies have described smart solutions based on the use of fisheye lenses (Covas et al., 2015; Perfetti et al., 2017), multi-cameras (Perfetti & Fassi, 2022), 360º cameras (Barazzetti et al., 2022) or low-weight cameras located on masts (Fiorillo et al., 2016; Pérez-García et al., 2019).

Traditionally, the study of the geometry of Egyptian funerary structures has been based on dimensions obtained from direct measurements based on tapes and laser distance meters (Martinez-Hermoso et al., 2015) or extracted from plans and sections obtained using surveying techniques and other sources (Rossi, 2001; Gardón-Ramos, 2021). These studies include the analysis of dimensions, proportions, etc. More recently, some studies have included the obtaining of 3D models, but results are more related to 3D documentation than to developing a complete geometrical analysis of the construction (Echeverría et al., 2019; Mozas-Calvache et al., 2020; Mandelli et al., 2021). In this study, we propose a more specific approach based on 3D models in order to develop a complete geometrical analysis of Egyptian tombs, which includes the study of dimensions, proportions, the flatness of walls, inclinations and orientations.

1.2. The Middle Kingdom burial structures of Qubbet el-Hawa

The necropolis of Qubbet el-Hawa (Fig. 1) is located on a hill situated on the west bank of the Nile River in Aswan. The necropolis is composed of more than 100 hypogea (Edel, 2008) excavated during several periods of ancient Egyptian history. The necropolis is distributed along the hill (adapted to its slope) on a level situated at an intermediate height (Fig. 1a). Among other cases, a set of Middle Kingdom tombs (QH31, QH32 and QH33) is situated in the central zone of the necropolis on a terrace of the terrain oriented to the southeast (Figs. 1a and 1b). These burial structures (QH31, QH32 and QH33), the object of this study, are dated from 1845 to 1773 BC (12th Dynasty, under the kings Senwosret II and Amenemhat III) and were used to bury some of the governors of Elephantine, their nuclear families and some prominent members of their households. They can be considered the most representative cases of the construction techniques developed in this period because of their great dimensions and their complex structures composed of several spaces, such as halls of pillars, corridors, vertical shafts and burial chambers. They were excavated one after the other considering a sequence from QH32, followed by QH31 and finally QH33 (Sánchez-León & Jiménez-Serrano, 2015; Martinez-Hermoso et al., 2018). Although these tombs are adjacent structures, this sequence contrasts with their situation in the necropolis because QH32 is located between the others (Fig. 1c). A preliminary chronology of these structures can be derived from the inscriptions and material documented during the last archaeological excavations developed by the University of Jaén (Spain) from 2008. The QH32 structure is dated to the reign of Senwosret II and although the

name of the owner has not been discovered yet, it has been suggested that it was the tomb of the governor Khema (Sánchez-León & Jiménez-Serrano, 2016). QH31 was constructed subsequently (between the reigns of Senwosret II and Senwosret III) and its owner was Sarenput II (Sánchez-León & Jiménez-Serrano, 2015), who was a grandson of another governor of Elephantine, Sarenput I (buried in the QH36 tomb located in the northern zone of the necropolis). QH33 was dated to the end of the reign of Senwosret III or the earliest years of Amenemhat III and it is suggested that the owner was Heqaib-ankh (Sánchez-León & Jiménez-Serrano, 2015). Additionally, in a secondary burial chamber located at the bottom of a vertical shaft was buried his step-brother Heqaib III (Sánchez-León & Jiménez-Serrano, 2015).
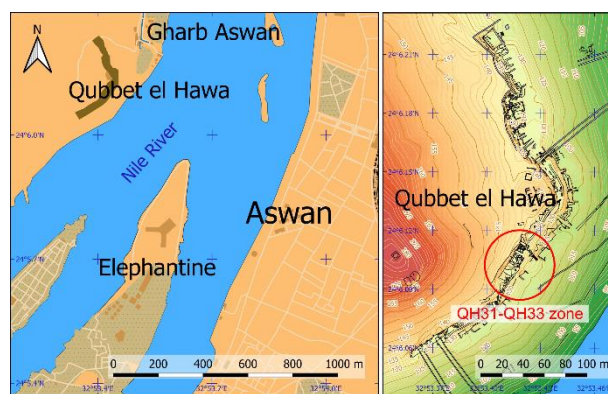
(a)

(b)

(c)

Figure 1: Situation of the burial structures QH31, QH32 and QH33: a) location of the necropolis; b) view of the necropolis; c) view of the entrances.

Although there are some differences between these structures, they present many similarities that can be

analysed in order to study their construction processes (Fig. 2). Firstly, they are composed of external (courtyard) and internal (hypogeum) zones. The courtyards were excavated on the slope, generating a façade that limited the external and internal zones. In all cases, the courtyard was supposed an accessing zone to each complex (Fig. 1c), but they were not completed due to a shortage of time caused (probably) by the sudden death of their owners or political changes (Martinez-Hermoso et al., 2018). Therefore, our objective is related to those internal zones. In this context, Table 1 summarises the main dimensions of these internal structures. The entrances to each hypogeum are separated by about 20 m (from QH31 to QH33) and QH31 and QH33 are located at a lower height level with respect to QH32 (Fig. 1c).

Table 1: Main dimensions of the QH31, QH32 and QH33 structures.

Tomb	Length (m)	Width (m)	Height (m)
QH31	32	23	18
QH32	22	13	9
QH33	23	10	18

(a)

(b)

(c)

Figure 2: Examples of burial structures analyzed in this study: a) QH31; b) QH32; c) QH33.

In each hypogeum, we must consider two parts: public space and burial area. The first was accessible and is composed of a hypostyle hall (containing several pillars), a corridor and an offering chapel (containing several pillars) where a sanctuary is located (Fig. 2). This distribution is quite similar in the case of QH31 and QH32. However, the QH33 tomb does not include a corridor and the sanctuary is integrated into the hypostyle hall. The second zone was inaccessible to the public and is composed of several corridors, chambers and vertical

shafts (up to 13 m in the case of QH33) that connected to the burial chamber where the deceased was buried (see examples in Fig. 2).

To summarize, in this study we analyse the geometry of these structures, including some aspects such as orientations, proportions and fitting to geometries using 3D models obtained by applying several geomatics techniques. The main objective is to analyse their architecture, trying to understand the construction processes of these burial complexes to discuss aspects such as planning, staking out and excavations.

2. Methodology and application

The methodology proposed in this study is summarised in Fig. 3. It is divided into three main stages: acquisition of data, processing and analysis. The main goal is to obtain several products and, derived from them, a set of results to analyse the geometrical behaviour of the burial structures, individually and together, in order to determine aspects related to the construction processes carried out in antiquity. The methodology includes the application of several geomatics techniques, such as TLS and CRP, to obtain a 3D documentation of the structure of each tomb and, derived from this product, determine several measures (dimensions and orientations) and analyse its geometrical behaviour. Thus, considering the usual complex structure of these scenes, we suggest the combination of TLS and CRP to obtain a complete 3D model of the tomb, although we could consider only one technique for this purpose. In this sense, the existence of narrow spaces and occlusions suggests the use of both techniques to avoid gaps in the final model. The application of both techniques must also include surveying work to determine the coordinates of several points (targets) which allows the global georeferencing of data. This stage is fundamental to analysing all burial structures altogether in the same coordinate reference system (CRS). Therefore, the acquisition of data is composed of three stages undertaken with three solutions, surveying, TLS and CRP.

The surveying work is carried out in two stages: firstly, a complete surveying network has to be implemented and measured in the exterior zone; secondly, this network has to be densified inside each tomb using a total station to allow the calculation of coordinates of the targets. An additional set of targets has also to be included to check all products geometrically (positional quality control).

The TLS survey includes the planning of scan stations to survey the full scene with a certain overlapping zone between adjacent stations in order to guarantee successful results of the registering stage. The density of scans must consider the requirements of the project and the average distances from scan stations to the object. We suggest capturing data without using the RGB acquisition mode of the scanner to improve the efficiency of the fieldwork. This option is justified when the texture of models is not demanded or if the texture will be obtained from CRP. Once all scans are obtained, the next stage consists of the registering of all point clouds to generate a total point cloud performing a relative orientation of all scans (considering a local reference system). Subsequently, a global transformation of the complete point cloud is carried out from the local reference system to a global one (e.g. CRS of the project). In this stage, we use some well-distributed points (targets) with known coordinates in the global CRS which are

measured in the registered point cloud. The last stage includes obtaining the definitive point cloud (TLS point cloud in Fig. 3) by filtering data and removing non-desirable points, such as those included in the scene that represents elements external to the object to be studied. The final TLS point cloud is checked geometrically by using several independent targets well-distributed throughout the scene.
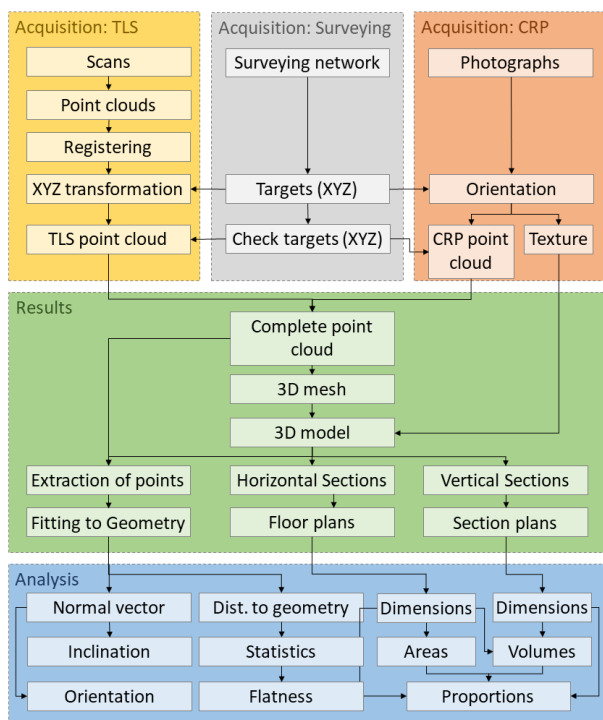

Figure 3: Methodology proposed in this study.

The CRP work includes the acquisition of photographs. Previously, we suggest a planning stage considering some aspects such as the features of the camera, distances to the object and illumination conditions. This previous analysis is carried out in order to ease the application of the recommendations of the CIPA Heritage Documentation for architectural photogrammetric projects using non-metric cameras (known as 3x3 rules) (Waldhäusl & Ogleby, 1994; CIPA, 2017). These rules include multiple photographic all-around coverage taking a ring of images around the object and overlapping each other by more than 60% (Waldhäusl & Ogleby, 1994; CIPA, 2017). We suggest the acquisition of normal-case photographs and convergent photographs covering the whole scene. The next stage consists of the orientation of photographs using applications based on algorithms such as SfM and MVS. The orientation is carried out using several targets included in images with known coordinates in the global CRS of the project. After the orientation, we obtain two products, a dense point cloud and a texture of the scene. The final CRP point cloud is checked geometrically by using several independent targets well-distributed throughout the scene.

Once both point clouds (TLS and CRP) are obtained, we obtain a combined point cloud adding a selection of CRP points to the TLS point cloud in zones without data. This complete point cloud is used to obtain a 3D mesh. The definitive 3D model uses this mesh and the texture previously obtained using CRP data.

The 3D model supposes a basic product to obtain reliable information about burial structures. In addition, the methodology includes obtaining several secondary products by extracting point clouds of significant elements (e.g. walls, ceilings and floors) and performing horizontal and vertical sections:

- The extraction of point clouds related to some elements (e.g. walls) allows us to determine geometries by fitting this set of data to geometrical elements such as planes, cylinders and spheres. In the case of the burial structures considered in this study, the majority of elements are planes because this is the main geometrical structure used in walls, ceilings and floors, although there are some ceilings where a fitting to cylinders is possible. The methodology proposes the use of the normal vector of the planes obtained to determine some geometrical aspects of each element (walls, floor, ceiling, etc.). In this sense, the normal vector of each geometry provides us with the inclination and orientation of the element. Thanks to these values we can analyse, for example, the verticality of a wall or the inclination of the ceiling. In addition, if we consider a set of walls that define the structure longitudinally or transversally we can obtain orientations of singular spaces or the complete structure. The determination of orientations (e.g. azimuth) will provide information on the possible definition of the tomb with respect to cardinal or astronomic directions. In this case, we have to consider the CRS used in order to determine directions to the north. As an example, the use of a cartographic projection such as the Universal Transverse Mercator (UTM) will suppose the calculation of the meridian convergence in order to obtain the azimuth from the true north instead of the cartographic north.

- The fitting procedure also provides other important information about the level of adjustment which has been achieved by the point clouds regarding the geometry. In the case of planes, this information shows us the level of flatness of walls. Thus, the distances between the points and the plane will inform us about the flatness of this element. In the case of cylinders, the distances between points and the cylinder will inform us about the skills of ancient builders in adjusting to this geometry. The information based on the distance to the geometry from a large number of points is used considering statistics such as the mean value of distance and the standard deviation of values. An ideal adjustment will provide null values of the mean distance value and null deviation. However, this supposes a utopic case which is not possible in reality due to the discrepancies in the construction and the errors caused by the data acquisition system. Once all the geometries are obtained, their interactions can be analysed by studying some aspects such as crosses, parallelism and perpendicularity. The determination of these geometries can also be used as basic information for performing a Building Information Modelling (BIM) project of the tombs or virtual reconstructions.

- Horizontal sections obtained from 3D models allow us to obtain floor plans at singular levels. From these products, we can obtain the lengths and areas of several elements of the burial structure, which can be used to compare elements and determine the

proportions of each element (internally) or between different elements.

- The application of vertical sections to the model allows the obtaining of section plans to determine length, areas and volumes (considering dimensions obtained from floor planes). These measures also allow the calculation of proportions to compare elements or relations inside each element. In addition, section plans also provide values of inclinations which can be used to study elements such as pillars and corridors.

The application of the methodology proposed in this study to real cases was carried out on three adjacent burial structures from the Middle Kingdom. More specifically, we developed several geomatic works in the QH31, QH32 and QH33 tombs (previously described). These studies are included in the framework of the project developed during the last decade by the University of Jaén (Spain) in the Necropolis of Qubbet el-Hawa. Thus, during several field campaigns, TLS and CRP techniques were applied to these burial structures. Data acquisition was carried out using a Faro Focus X130 terrestrial laser scanner and

a Sony Alfa 5000 digital camera. We used Faro Scene v. 2020 (for TLS) and Agisoft Metashape v. 1.6 (for CRP) software to process data. Georeferencing of the data was based on a set of targets distributed over the walls. We also controlled intermediate and final products using an independent set of targets. The coordinates of both sets of targets were obtained using a total station. We obtained accuracies below 1 cm in each case and discrepancies between both models (TLS and CRP) below 2 cm. A more detailed description of this application is given by Mozas et al. (2020). Once a 3D model of each structure was obtained, several point clouds which represent walls, ceilings and floors were extracted. These point clouds were fitted to planes and cylinders. We used Maptek Point-Studio v. 2020 and CloudCompare v. 2.11 software to determine planes and cylinders, the normal vector and the values of the distances. The orientation and inclinations were calculated directly from the normal vector using a spreadsheet. On the other hand, horizontal and vertical sections were obtained using Maptek Point-Studio software. After that, floor plans and section plans were developed using Autodesk AutoCad v. 2019 software.

(a)

(b)

(c)
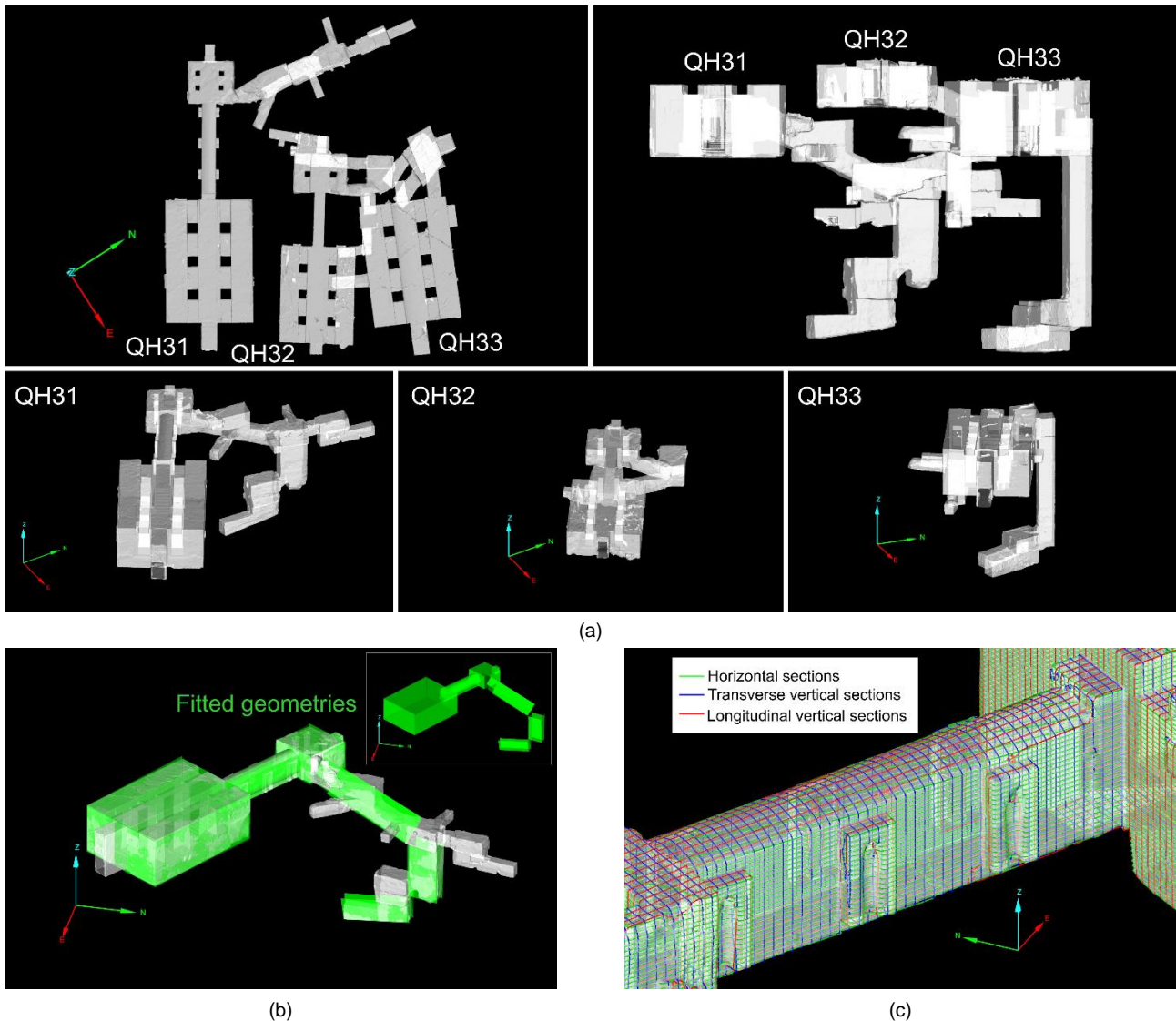
Figure 4: Results obtained: a) 3D models of the burial structures; b) geometries fitted to extracted point clouds; c) horizontal and vertical sections.

3. Results and analysis

The first results of this study are related to three 3D models of the three burial structures (Fig. 4a). These models show an incredible closeness between the structures reaching, in the case of QH32 and QH33, a minimum value of 10 cm without intersections (Mozas et al., 2020). Using these 3D models we have calculated the volumes of excavation showing values of 646.8, 295.1 and 588.5 m^3 (QH31, QH32 and QH33). These volumes reflect the magnitude of the excavation works carried out in building these complexes in antiquity.

Considering the methodology proposed in this study, we have extracted several point clouds from different elements, such as walls, floors and ceilings, and we have fitted these point clouds to several geometries, such as planes and cylinders (Fig. 4b). In addition, we have also generated horizontal and vertical sections (Fig. 4c). Considering these sections, we have obtained several plans such as those displayed in Fig. 5 and Fig. 6. All these results allow us to analyse some geometrical aspects such as dimensions and orientations, which are described in the following sections.

A: Entrance; B: Hypostyle hall; C: Corridor; D: Cult chamber; E: Sanctuary; F: Descending corridor; G: Antechamber; H: Vertical shaft; I: Funerary chamber; J: Niche

Figure 5: Plans of the burial structures analysed in this study.
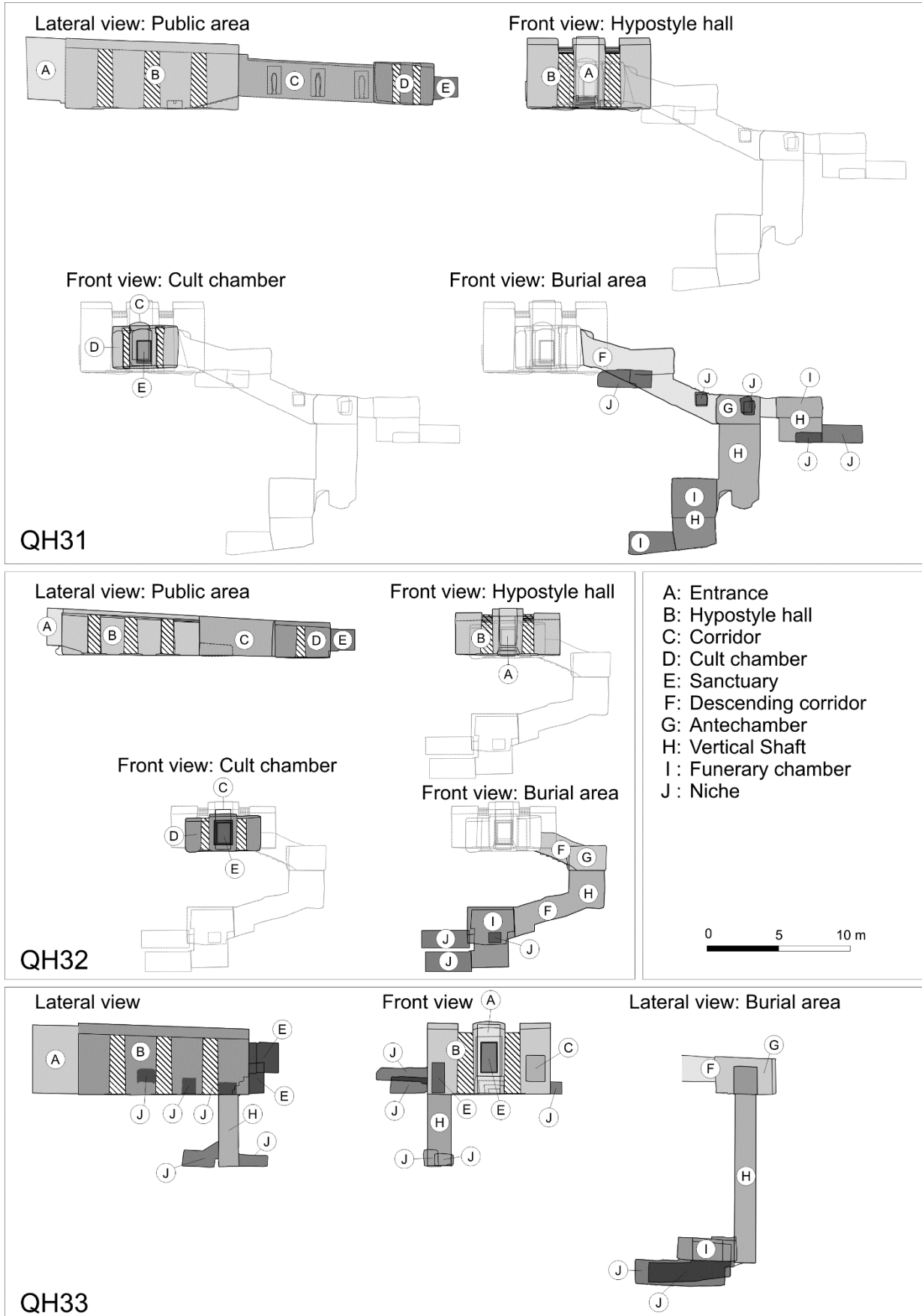
Figure 6: Plans of the burial structures analysed in this study.

3.1. Dimensions

A basic visual analysis of the plans displayed in Fig. 5 (top views) and Fig. 6 (sections) shows several similarities between all of the tombs. Hence, both the public and the burial areas have common spaces in all structures analysed in this study, although in the case of the public areas the similarities of geometrical aspects are highlighted. As an example, the hypostyle halls (B in Fig. 5) are structured by a rectangular area divided into three naves separated by two rows of three pillars (six in total). The main dimensions of the structures are shown in Table 2 grouped by parts or spaces from the entrance to the funerary chamber. These values are shown in meters but also in ancient Egyptian units and more specifically in royal cubits, palms and fingers (c, p, f, in Table 2). Considering the available literature about these units and some examples of remains of cubit rods discovered in several archaeological sites, we have considered one royal cubit to be about 0.524 m, which are divided into seven palms (one palm is about 0.075 m) and each palm is divided into four fingers (one finger is about 0.019 m). The first conclusion of the results shown in Table 2 is that QH32 presents lower dimensions than the other tombs. The entrances (part A) show a coincidence of width in QH31 and QH33 of about 1.6 m (3 c), while the remaining dimensions are greater in QH33 with respect to the other (3.2 m x 1.6 m x 4.8 m, 6 c x 3 c x 9 c approximately). Clearly, the size of the entrance is related to the dimensions of the tomb.

In the case of the hypostyle halls (part B in Table 2), the dimensions are quite similar in the QH31 and QH33 tombs, although QH31 shows a greater reduction of height from the entrance to the corridor than QH33. This aspect causes a higher volume of QH33 with respect to that obtained in QH31 in spite of the greater area of QH31. The reduction of height with the distance from the entrance is common in hypostyle halls. In this sense, the ceilings show inclinations of about 3.7% (QH31), 4.4% (QH32) and 0.7% (QH33) (see initial and final height in Table 2). Another important aspect of this space is related to the dimensions of the pillars. The average length and width obtained from each set of 6 pillars of each tomb shows 1.13 x 1.14 m (at the bottom) and 0.99 x 1.01 m (at the top) in the case of QH31, 0.94 x 0.83 m (at the bottom) and 0.84 x 0.74 m (at the top) in QH32 and 1.11 x 1.14 m (at the bottom) and 1.00 x 1.03 m (at the top) in QH33. In all cases, the pillars show a reduction of the section with the height. In the case of QH31 and QH33, the dimensions (both at the bottom and the top) are quite similar (sides of about 1.1 m, 2 c) as happened with the dimensions of the hypostyle halls.

Table 2: Dimensions of the main parts of the burial structures: A: entrance; B: hypostyle hall; C: corridor; D: cult chamber; E1: sanctuary (complete); E2: sanctuary (interior); H: vertical shaft; I: Funerary chamber.

	Tomb	Length m (c p f)	Width m (c p f)	Initial Height m (c p f)	Final height m (c p f)	Area (m²)	Volume (m³)
A	QH31	2.70 (5c 1p)	1.58 (3c)	4.61 (8c 5p 2f)		4.3	19.7
	QH32	1.12 (2c 3f)	1.29 (2c 3p)	2.60 (4c 6p 2f)		1.4	3.7
	QH33	3.21 (6c 3f)	1.59 (3c)	4.77 (9c 2f)		5.1	24.3
B	QH31	12.08 (23c 1f)	8.59 (16c 2p 3f)	4.91 (9c 2p 2f)	4.46 (8c 3p 2f)	103.8	486.1
	QH32	9.58 (18c 1p 3f)	7.22 (13c 5p 1f)	3.28 (6c 1p 3f)	2.86 (5c 3p)	69.2	212.3
	QH33	11.91 (22c 5p)	8.57 (16c 2p 1f)	4.90 (9c 2p 1f)	4.81 (9c 1p 1f)	102.1	495.5
C	QH31	9.43 (17c 6p 3f)	1.42 (2c 4p 3f)	2.65 (5c 1f)	2.61 (4c 6p 3f)	13.4	35.2
	QH32	5.27 (10c 1f)	1.10 (2c 2f)	2.74 (5c 1p 2f)	2.5 (4c 5p 1f)	5.8	15.2
D	QH31	4.21 (8c)	4.59 (8c 5p 1f)	2.97 (5c 4p 2f)		19.3	57.4
	QH32	3.99 (7c 4p 1f)	5.24 (10c)	2.45 (4c 4p 2f)		20.9	51.2
E1	QH31	1.68 (3c 1p 1f)	1.03 (1c 6p 3f)	1.61 (3c 0p 2f)	1.44 (2c 5p)	1.7	2.5
	QH32	1.70 (3c 1p 2f)	1.03 (1c 6p 3f)	1.54 (2c 6p 2f)	1.42 (2c 4p 3f)	1.7	2.5
	QH33	2.06 (3c 6p 2f)	1.17 (2c 1p 2f)	2.13 (4c 0p 1f)	2.05 (3c 6p 1f)	2.4	4.9
E2	QH31	1.15 (2c 1p 1f)	0.95 (1c 5p 2f)	1.44 (2c 5p)		1.1	1.6
	QH32	1.16 (2c 1p 1f)	0.95 (1c 5p 2f)	1.42 (2c 4p 3f)		1.1	1.6
	QH33	1.54 (2c 6p 2f)	1.04 (1c 6p 3f)	2.05 (3c 6p 1f)		1.6	3.3
A-E	QH31	30.10 (57c 3p)				142.5	600.9
	QH32	21.66 (41c 2p 1f)				99.1	285.0
	QH33	17.18 (32c 5p 2f)				109.6	524.8
H	QH31	2.85 (5c 3p)	1.48 (2c 5p 3f)	5.19 (9c 6p 1f)		4.2	21.9
	QH32	2.32 (4c 2p 3f)	1.06 (2c)	2.59 (4c 6p 2f)		2.5	6.4
	QH33	1.56 (2c 6p 3f)	1.55 (2c 6p 2f)	11.73 (22c 2p 2f)		2.4	28.3
I	QH31	3.15 (6c)	2.21 (4c 1p 2f)	2.78 (5c 2p)		7.0	19.3
	QH32	3.41 (6c 3p 2f)	3.07 (5c 6p)	2.6 (4c 6p 2f)		10.5	27.2
	QH33	3.21 (6c 0p 3f)	3.61 (6c 6p)	1.56 (2c 6p 3f)		11.6	18.1

The corridors (part C in Table 2) connected the hypostyle halls and the cult chambers of QH31 and QH32. The dimensions of these spaces follow the previously-commented tendency with a significative reduction of length and width in the case of QH32 with respect to QH31. However, the height is similar in both cases, although QH32 shows a more notable reduction of height between the start of the corridor and the end. The corridors have lengths of about 9.4 m and 5.3 m (18 c and 10 c) and widths of about 1.4 m and 1.1 m (2 c 4 p and 2 c) respectively (QH31 and QH32).

The cult chambers (part D in Table 2) are included in QH31 and QH32 to contain the sanctuary, while QH33 connects this space directly to the hypostyle hall using a stairway. The dimensions of the cult chambers are very different in both cases, although the widths are greater than the lengths. QH31 shows a larger cult chamber including four pillars, while QH32 only contain two pillars. In this sense, the section of the pillar is greatest in the case of QH32 (about 0.6 m in contrast to 0.5 m in QH31).

The sanctuary (part E in Table 2) supposes to be a main space of the burial structure and this aspect is clearly justified by its prominent location inside the public area. In addition, all sanctuaries are decorated with paintings in which the owner of the tomb appeared. In this case, the dimensions of the sanctuaries of QH31 and QH32 are quite similar (length, width and height). Logically, this similarity is also shown by the results of area and volume. However, the sanctuary of QH33 is larger than the other two, with a square determined by the length and the height (about 2 m, 3 c 6 p). One hypothesis can be that this increase in dimensions can be related to the fact that QH33 does not contain a cult chamber, and this space is also annexed to the sanctuary. On the other hand, the finality of this space, which included a statue of the owner, could also justify this increase in dimensions. Considering this hypothesis, the statue of QH31 had to be larger than the rest, although there is no evidence of this at the moment.

Therefore, considering all the public spaces (A-E), we obtained lengths of about 30.1 m, 21.6 m and 17.2 m (57 c, 41 c and 33 c) respectively. Logically, the presence of corridors (C) and cult chambers (D) in the cases of QH31 and QH32 supposes a lengthening of the public space with respect to QH33.

As we have described, the public area shows great similarities between the tombs analysed in this study. However, the burial area does not present the same behaviour. All cases show different spaces such as corridors, vertical shafts, burial chambers and niches but we cannot find coincidences between the situation and dimensions of these structures in spite of the fact that these spaces start with a corridor that is situated in the northern part of the public area. The addition of several burial structures which are adjacent to the main one, dedicated to other members of the governor's family, complicates the structure of the burial zone. To summarize, our study of dimensions has centred on the main vertical shaft (H) and the funerary chamber (I), although the plans displayed in Figs. 5 and 6 allowed us to carry out a more complete analysis of the rest of the structures. Thus, in the case of QH31 and QH32 a descending corridor is located contiguous to the cult chamber and after that, a vertical shaft and another corridor connected to the main funerary chamber. In the

case of QH33, the corridor is shorter than in the other cases, but the vertical shaft is the largest one (more than 11.7 m; 22 c) (Table 2). In the case of QH31 and QH32, the vertical shafts have a rectangular ground plan while QH33 shows a squared one (almost 1.6 m; 3 c).

The funerary chambers show irregular structures from where the main niches are located. In general, they can be described as spaces with a rectangular plan and variable height. In this case, QH31 shows reduced dimensions with respect to the rest. As is displayed in Fig. 5, the funerary chamber and more specifically, the main niches of QH32 and QH33 are located several meters along the vertical line below the sanctuary.

3.2. Proportions

The dimensions of the structures described in the previous section have evidenced the existence of great spaces excavated inside the hill. These values have demonstrated the advanced skills achieved by ancient Egyptians in construction techniques, which is also confirmed when we analyse the proportions and orientations of these tombs.

In this sense, we have confirmed the existence of defined proportions between the dimensions of some elements as well as between several spaces of these structures. The existence of these proportions demonstrates the planning carried out previously to the construction and the great precision achieved in the construction works. In addition, some of these proportions are common to spaces of some tombs, indicating that these ratios were considered in several burial structures although they were constructed during different periods.

Table 3 shows a set of ratios that suggests the existence of proportions considering relations such as Length/Width, Length/Height and Width/Height in some elements of the tombs. This is the case of the entrance, in which ratios between Length/Width and Length/Height are related to √3 in the case of QH31. In the case of QH33, the ratios are related to 2 and 1/3.

Table 3: Main proportions detected in the tombs.

	Tomb	L/W	L/H	W/H
A	QH31	√3	1/√3	1/3
	QH32	2/√3		0.5
	QH33	2	1/3+1/3	1/3
B	QH31	√2	2.5	√3
	QH32	1+1/3		2.5
	QH33	√2	2.5	√3
E1	QH31	2*√2/√3	2/√3	1.5
	QH32	2*√2/√3	√3/√2	1.5
	QH33	√3	1	1/√3
E2	QH31	√3/√2	1.25	1.5
	QH32	√3/√2	√3/√2	1.5
	QH33	1.5	1+1/3	
A+B+C+D+E	QH31	3.5		
	QH32	3		
A+B+E	QH33	2		

The hypostyle halls show a Length/Width ratio of √2 (QH31 and QH33) and 1+1/3 (QH32), Width/Height ratios of √3 (QH31 and QH33) and 2.5 (QH32) and a Length/Height ratio of 2.5 (QH31 and QH33). Therefore, the hypostyle halls of QH31 and QH33 have similar proportions. The sanctuaries also show some common proportions in their dimensions. In this case, we have divided the analysis considering the complete space (E1) and the interior part (E2) of each sanctuary. Thus, the sanctuaries of QH31 and QH32 show approximately similar values for all of the ratios analysed, which are related to √2 and √3, while QH33 shows other ratios related to √3.

Finally, the complete analysis of proportions of the public spaces (A-E) shows interesting results because the Length/Width ratio shows values of 3.5, 3 and 2 respectively. This supposes that public areas were constructed considering a relationship between the length and the width, this width being that defined by the largest element, which is the hypostyle hall in all cases. Figure 7 confirms this aspect when we consider the semi-width of the hypostyle hall as a proportional value that defines the structure and distribution of the public area. Thus, QH31 shows that the length of the public space is equal to 7 times its proportional value (4.3 m, 8c 1p), QH32 shows 6 times its proportional value (3.61 m; 6c 6p) and QH33 shows 4 times its proportional value (4.29 m, 8c 1p). The proportional value allows the main elements of these tombs to be distributed following the schema shown in

Fig. 7 (e.g. the pillars of the hypostyle hall of QH33). In addition to this distribution, some elements show dimensions related to the proportional value. For example, the height of the sanctuary (E) in the case of QH31 (ratio 1/3) and QH33 (ratio 1/2). To summarize, the study of proportions demonstrates that the construction of these structures was planned previously and executed with great accuracy, attempting to apply an artistic sense of harmony.

3.3. Fitting to geometries: flatness, orientations and inclinations

The 3D model of the structure has allowed us to adjust several geometries to walls, ceilings and floors. More specifically, in this study, we have used a selection of points extracted from the model to calculate a fitted geometry related to planes or cylinders and we have analysed the results of the adjustment. Figure 8 shows some examples of calculated fitted geometries and the distances from point clouds to these geometries. As an example, Figs. 8a and 8b show the results of the fitting of the vaulted ceiling of the corridor to a cylinder (Fig. 8a) in the case of QH31. The fitted cylinder has a length of 8.78 m and a radius of 1.19 m. The distances between the point cloud and the fitted cylinder show values of up to 0.062 m (histogram displayed in Fig. 8b). This graphical representation of distances allows us to analyse the quality of the adjustment and the deviation of the reality (point cloud) with respect to the ideal geometry
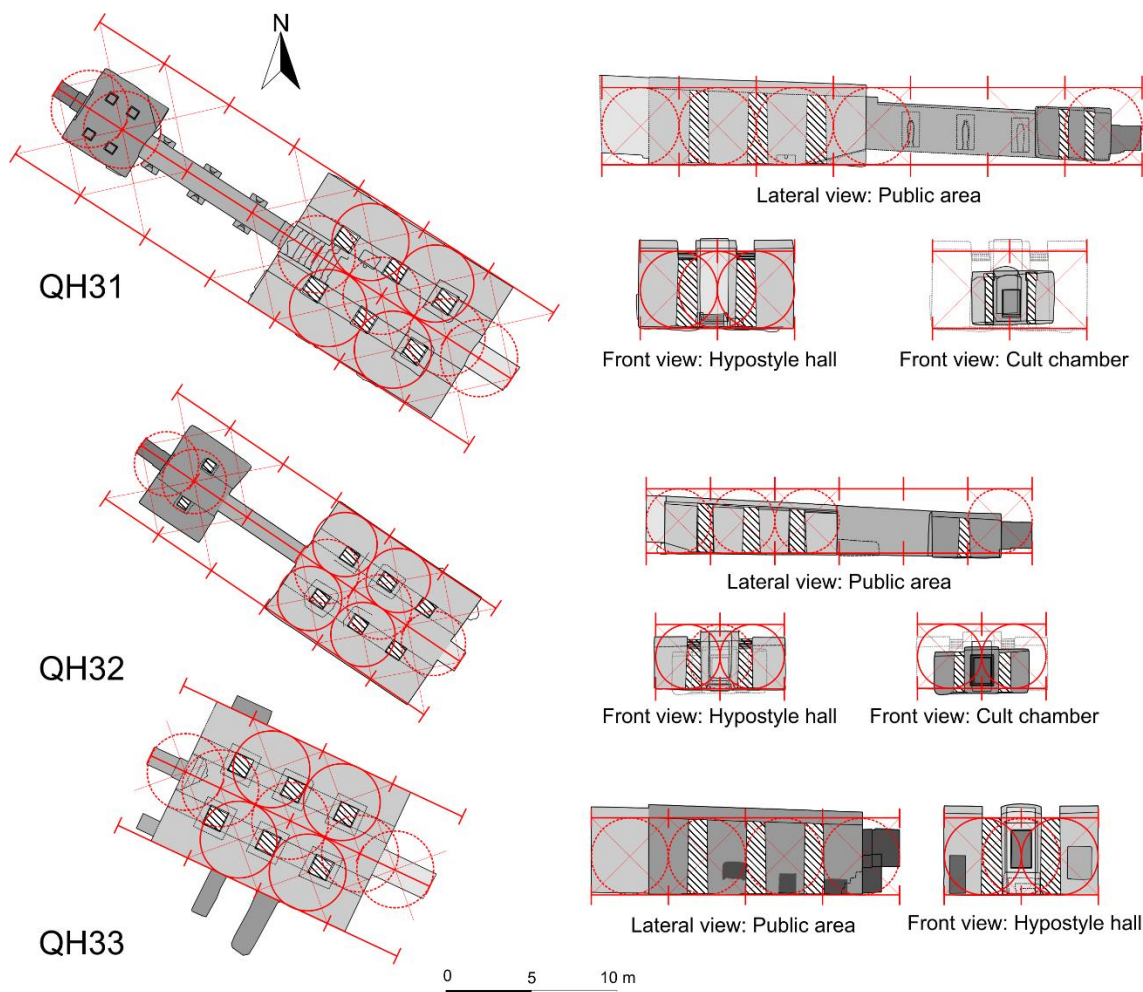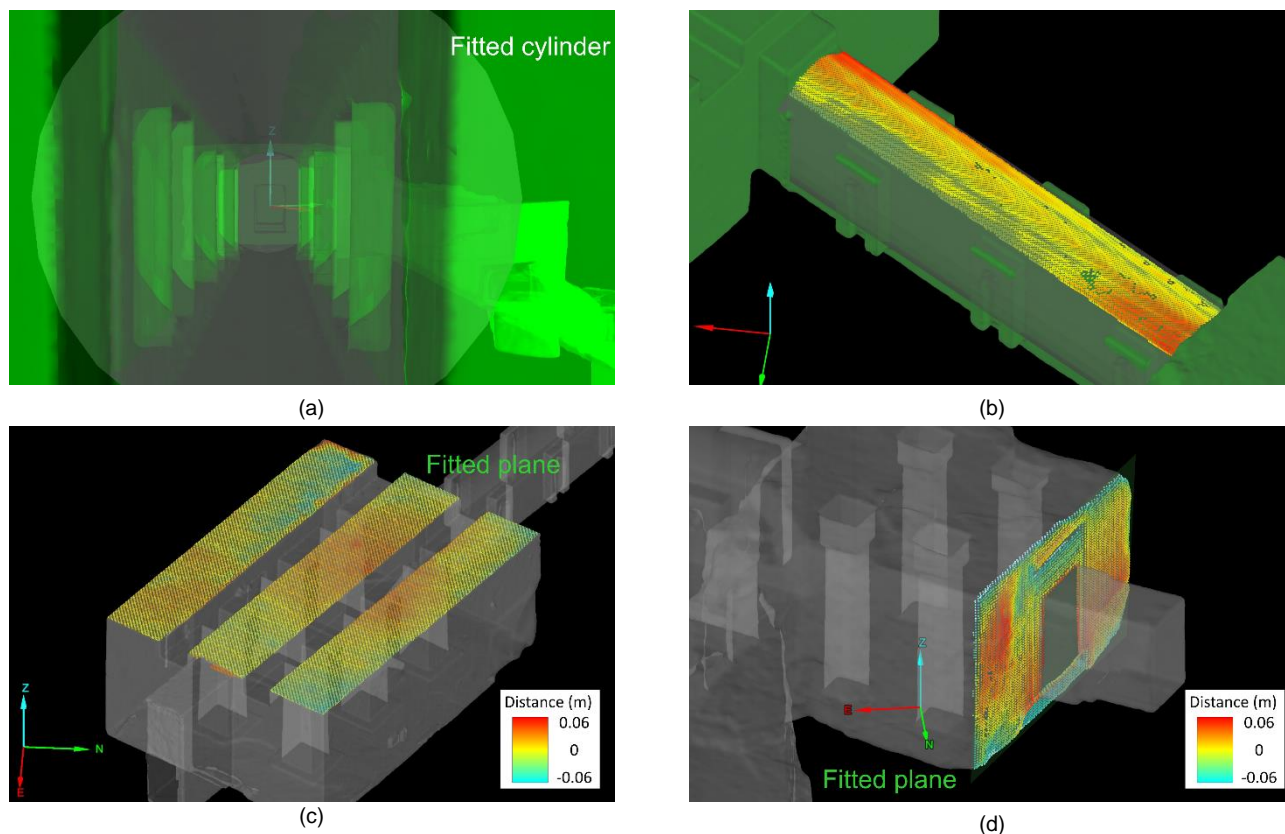

QH31

QH32

QH33

Lateral view: Public area

Front view: Hypostyle hall   Front view: Cult chamber

Lateral view: Public area

Front view: Hypostyle hall   Front view: Cult chamber

Lateral view: Public area   Front view: Hypostyle hall

0   5   10 m

Figure 7: Proportions detected in the tombs related to the semi-width of the hypostyle hall.

Figure 8: Examples of fitted geometries and analysis of distances from point clouds (QH31): a) fitted cylinder of the vaulted ceiling of the corridor; b) distances between points and cylinder (corridor ceiling); c) distances between points and plane (hypostyle hall ceiling); d) distances between points and plane (offering chamber frontal wall).

(plane or cylinder). In addition to these graphical representations which are related to specific elements, and in order to study the spaces altogether, we have also used some statistical measures. The goal is to analyse the distances from the points to the fitted geometry based on measures such as the mean distance and the standard deviation.

Considering these measures, we have grouped the results of walls, floors and ceilings of each element by the tomb, obtaining the graphics shown in Fig. 9. In general, the mean distances are close to zero in a large number of cases but some exceptions are also displayed (e.g. walls of zone F in QH31). On the other hand, the values of standard deviation show the dispersion of distances with respect to the mean value. We suppose that a good adjustment is that which shows a mean value of zero and a low value of standard deviation (lower than 0.01 m). This supposes that distances do not present bias and distances are reduced with respect to the fitted geometry. As an example of this case, the walls of zone B of QH33 can be considered flat walls. A second case is that with a mean value of zero and a higher value of standard deviation (between 0.01 and 0.02 m). In these cases (e.g. walls of zone I of all tombs), distances from points to the fitted geometry do not show bias, but the distances show higher values and variability. This is a clear example of rough walls. Therefore, this analysis can be used to estimate flatness in the case of planes. Finally, the case of mean values different to zero supposes the existence of a bias in distances. A histogram of distances shows clearly the presence of bias, such as the example of the corridor (zone C) of QH31 shown in Fig. 8b. These cases are usually displayed with large values of standard deviation (Fig. 9).

This supposes a poor adjustment of points to the geometry caused by an irregular excavation originally or the existence of zones which have subsequently collapsed. For example, the walls of zone D in QH31 show poor adjustments to planes. These cases are also shown in the case of the ceiling of zone B in Fig. 8c and the frontal wall of zone D shown in Fig. 8d.

Considering the results shown in Fig. 9, the best adjustment is related to the public zones and more specifically to zones A, B and E.

The study of orientations of the elements of the burial structures is based on values of azimuths obtained from the previously-obtained fitted planes. Thus, in each space of the tomb, there are two planes that define the orientation of this element (considering the two walls of the greatest length). The orientation of each plane is obtained using the normal vector which defined it. The definitive orientation of space is obtained by the average value obtained from both opposite planes. Finally, we applied a calculated value of the meridian convergence in order to obtain the direction to the true north (azimuth). To summarise, Table 4 shows the main values of orientations of the different spaces of the tombs. The public spaces are approximately oriented following a straight line. All cases show similar orientations with azimuths from 115 degrees (QH33) to 123º (QH32). The first orientation is related to the sunrise of the winter solstice at this latitude (Shaltout & Belmonte, 2005). In contrast to these data, the funerary spaces show more variability of orientations. Thus, the only coincidence between spaces is related to the vertical shaft of QH31 and QH33. In both cases, the values of azimuths are about 190º. The values of orientation obtained using this methodology have been
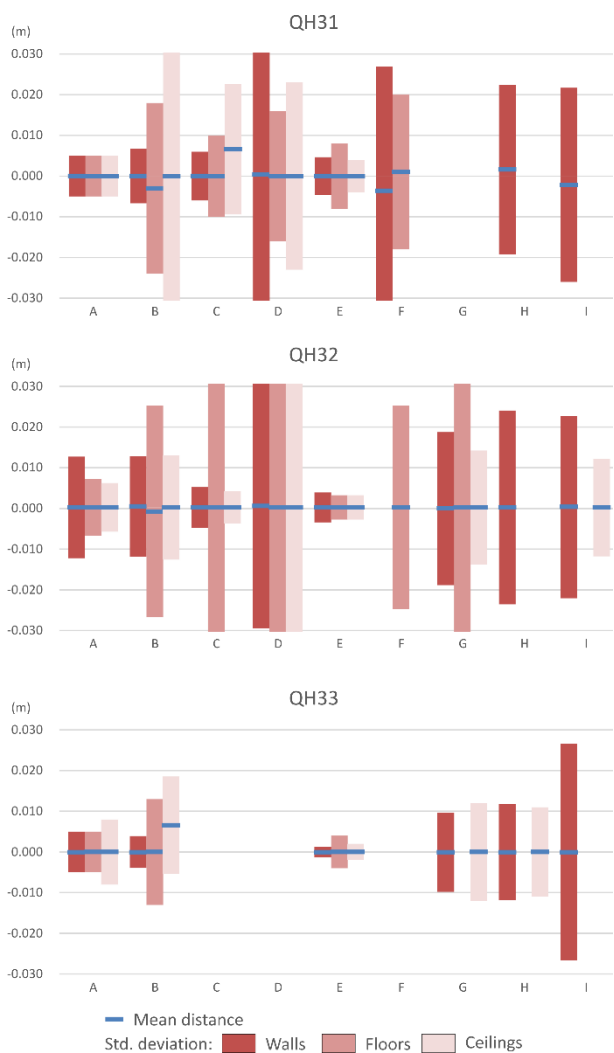
Figure 9: Statistics of distances from points to fitted geometries.

Table 4: Main orientations detected in the tombs.

	Tomb	Degrees	Minutes	Seconds
A	QH31	122	32	12
	QH32	125	19	28
	QH33	114	58	36
B	QH31	121	57	1
	QH32	123	54	6
	QH33	114	57	9
C	QH31	122	51	38
	QH32	124	6	17
D	QH31	123	5	23
	QH32	125	10	59
E	QH31	123	14	16
	QH32	126	19	34
	QH33	114	52	31
H	QH31	193	23	45
	QH32	212	50	45
	QH33	191	39	19
I	QH31	182	50	55
	QH32	220	8	8
	QH33	160	28	51
A+B+C+ D+E	QH31	122	31	9
	QH32	124	27	4
A+B+E	QH33	114	56	52

checked in some singular cases using a total station showing minimum discrepancies (e.g. differences of about 20' in the case of zone B of QH33) (Joyanes-Díaz et al., 2022).

The verticality and horizontality of fitted planes are also analysed in this study grouped by spaces and individually. Figure 10 shows the results of inclinations grouped by element considering walls, floors and ceilings. In the case of walls, the best results of verticality are shown in public spaces and more specifically in the hypostyle halls (A), the corridors (C) and the sanctuaries (E) with values that are close to 90º. However, other cases show greater inclinations of walls, such as in the case of the descending corridor (F) of QH31 where the inclination angle is lower than 88º. Our data confirm that the walls of public spaces were excavated with great accuracy that could have been reached by using several tools to hit the rock, such as chisels, and instruments to guarantee verticality, such as square levels, plummets, etc. In addition, they could also have used some excavation techniques (e.g. abrasive sand) to polish the walls, achieving a remarkable degree of flatness. A more detailed description of tools used in ancient Egyptian construction is given by Harrell (2008).

The analysis of the inclination of floors or ceilings must consider that, in most cases, these elements are intentionally executed with a certain inclination. Therefore, the inclination of the geometry must only be considered as a feature of the element but without assessing the quality of execution of the excavation. Thus, an example of floors with a certain inclination is that related to sanctuaries, which achieved almost one degree in the case of QH33. Another case to highlight is that related to the descending corridors (F) of QH31 and QH32, which show values of 26º and 23º respectively. On the other hand, the floor of the hypostyle hall of QH33 shows a great horizontality with an inclination of hardly 0.1º. In the case of ceilings, we highlight the inclination of the ceilings of the hypostyle halls (B), which achieved 3º in the case of QH32 and the sanctuaries (E) where QH33 shows the greatest inclination of about 3.1º. In contrast, the ceiling of the sanctuary (E) of QH32 only shows an inclination of 0.4º.

In addition to the general analysis of verticality and horizontality by spaces described previously, we have also analysed each fitted geometry individually. Thus, we have obtained values of inclinations for walls, floors and ceilings, analysing them graphically. In this sense, Figure 11 shows the values of inclinations of the fitted planes of the walls of QH31. The inclinations obtained have been divided into 5 intervals to show the behaviour of this variable distributed throughout the burial structure. It is clear that the verticality of planes was an important aspect taken into account by ancient Egyptians in several spaces

such as entrances, hypostyle halls, corridors and sanctuaries. However, the funerary spaces do not present behaviours as fine as the public ones.
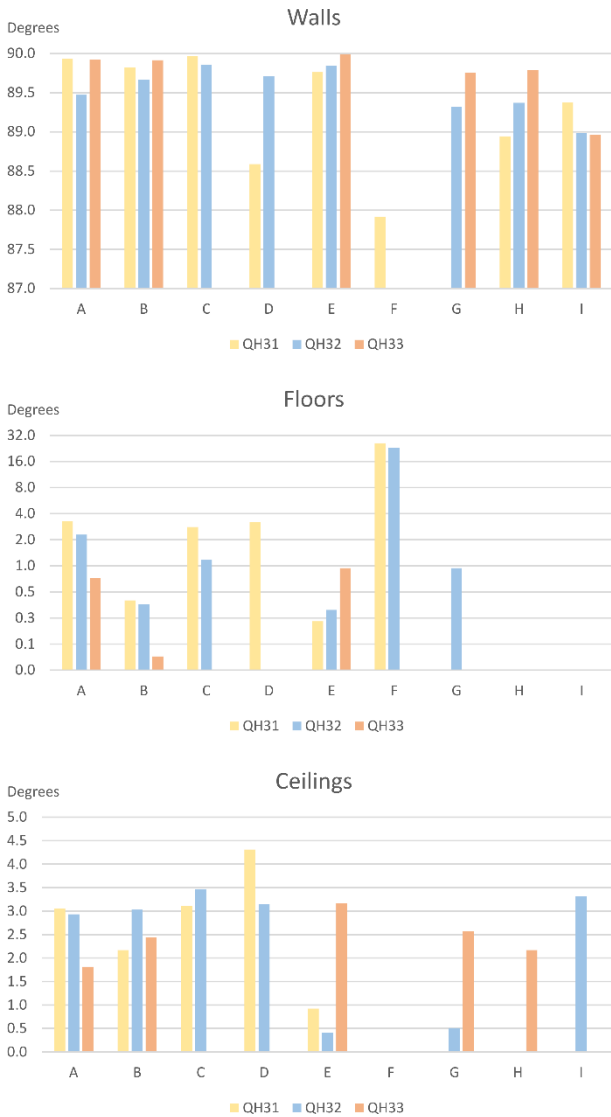
Walls

Floors

Ceilings

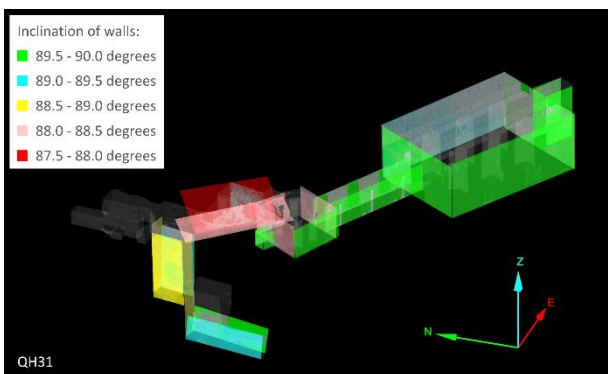**Figure 10**: Inclinations of fitted geometries.

Figure 11: Inclinations detected in the walls of QH31.

4. Discussion

The results of the geometrical analysis obtained in this study show interesting aspects to confirm the incredible constructive skills of ancient Egyptians. In this sense, the methodology applied in this study, based on 3D models,

has allowed us to obtain a large amount of data about the geometry of the burial structures analysed. The analysis is based on products derived from the 3D models, such as plans and sections, used to analyse dimensions, areas, volumes and proportions, and fitted geometries obtained from point clouds that define different elements of the burial structures (walls, floors and ceilings).

The study of dimensions, area and volumes has allowed us to obtain basic information about the structure of each tomb and a comparison between data of similar spaces in them. This allows us to establish an evolution in the structures considering their estimated date of construction. Thus, evolution is clearly defined from QH32 (the first tomb constructed), QH31 and QH33, which we consider the most evolved one. In this sense, QH32 shows the most reduced dimensions of common elements while QH33 shows the greatest hypostyle hall (quite similar to QH31), the greatest sanctuary and the largest vertical shaft although this tomb does not contain a corridor and cult chamber. In this case, we consider the cult chamber to be integrated into the hypostyle hall. On the other hand, it is remarkable that the structure of the public area of QH32 and QH31 are quite similar, considering an increase in dimensions of all elements although the sanctuaries show similar dimensions. We suppose that QH31 was planned and executed following the experience achieved after QH32. Along the same line, we suppose that the structure of QH31 was considered in the development of QH33 because the dimensions and structure of the hypostyle hall are quite similar, although the presence of QH32 limited the expansion of this structure to the interior and this supposed the removing of the corridor and the cult chamber.

The analysis of proportions detected in each element and their comparison with other elements of the same tomb and the other burial structures have shown amazing data. Firstly, we have detected several common proportions, such as $\sqrt{2}$ and $\sqrt{3}$ in different elements. In our opinion, this supposes the necessity of a previous planning of the structure and the accurate execution of the excavation tasks, but also the search for harmony of constructors and the mixture of art with architecture. In addition, the most notable results are those related to the existence of a proportion value at each tomb that defines the structure of the public area and the distribution of elements. This proportion value is related to the semi-width of the hypostyle hall of each tomb. It is remarkable that the lengths of the public areas are multiples of the proportion value in all cases (7, 6 and 4 respectively). This value acts in these structures similar to the widely known Egyptian canon, which defines human figures in Egyptian art. The use of data extracted from 3D models supposes an improvement with respect to traditional studies based on measures obtained directly in the field with tapes or laser distance meters because of the possibility of measuring as many times as necessary and of defining sections that allow us to obtain projected plans where dimensions are easily extracted.

The analysis of flatness, orientation and inclination of elements have been based on fitted geometries obtained from point clouds extracted from the 3D models. Firstly, the analysis of flatness is based on distances from points to the fitted planes. We have suggested the use of statistical measures of these values, such as the mean and the standard deviation. In this case, walls of the hypostyle halls, corridors and sanctuaries show the greatest level of flatness, with deviations lower than one

centimetre. Other walls were excavated roughly showing higher deviations. Logically, we suppose that the level of flatness is related to the importance of the element in the tomb. In addition to determining the level of flatness, this analysis based on statistical measures can be used to detect some zones inside elements that do not adjust to the fitted geometry correctly. A more specific analysis can be carried out using a graphical representation of distances such as those examples shown in Fig. 8. The study of orientations of the fitted geometries allows us to obtain the azimuth of the different spaces. This can be used to determine the general orientation of the tomb (based on the alignment of the public spaces). In this sense, we have found reduced deviations between elements which are supposed to be aligned (public spaces) and general alignments that are included in the interval from 114 to 124º. In the case of QH33, the azimuth obtained is related to the sunrise of the winter solstice. The study of verticality has demonstrated that ancient Egyptians had amazing skills enabling them to achieve the verticality of walls. Thus, a large part of the planes obtained from different elements of the public area has shown inclinations lower than 0.5º. This supposes an extreme deviation of less than one centimetre per meter. In the case of the walls of hypostyle halls and sanctuaries, the inclinations are reduced, with values of about 0.25º (4mm of deviation per one meter). However, some walls related to burial areas have shown greater inclinations (up to 2º). We suppose that these spaces are not as important as those to be visited. This hypothesis is confirmed by data regarding flatness because the level of flatness is greater in public spaces concerning burial ones. The analysis of inclinations based on fitted geometries allows us to study other horizontal or inclined elements such as floors, ceilings and ramps.

To summarise, the analysis derived from products extracted from 3D models has demonstrated the viability of the methodology proposed for developing a complete geometrical study of this type of burial structure (hypogea).

5. Conclusions

This study has described a methodology for developing a geometrical analysis of burial structures. In this context, this approach includes the acquisition of data, based on geomatics techniques, the obtaining of products (mainly 3D models) and the analysis of geometrical aspects such as dimensions, proportions, flatness, orientations and inclinations. The application of the methodology proposed in this study has demonstrated the viability of this type of analysis for detecting some important aspects of these burial structures and the constructive procedures carried out almost four millennia ago.

The analysis of dimensions has confirmed the great excavation volume reached in these tombs. In addition,

some elements of different tombs have similar dimensions, which implies that previous constructions were used as a pattern to develop subsequent structures. This aspect confirms the existence of previous planning. In this sense, the most amazing example is the absence of intersections between tombs in spite of the great closeness detected in several zones (e.g. between QH32 and QH33).

In this context, the analysis of proportions has revealed the presence of common ratios used to define some elements, including similarities between several tombs. This indicates that tombs were planned (previously to their execution) considering some specific proportions and even the experience of previous constructions, because ratios are repeated in several tombs. On the other hand, the inclusion of a proportion value which defined the structure and distribution of all tombs is very important if we consider a search for artistic harmony in constructions. This study has demonstrated the existence of planning and execution of tombs using these proportion values, which act as a canon to define their structure. Until this moment we have known about the Egyptian canon applied to human figures in art, but we have not had references to a similar grid used to develop Egyptian tombs.

The geometrical study described based on fitted geometries has allowed the obtaining of data about the flatness of planes, orientations of elements and structures and inclinations of elements. This analysis is not carried out in these types of structures by other studies based on data measured using tapes or laser distance meters. In this case, we have detected a high degree of flatness in walls related to main public spaces, such as those of hypostyle halls and sanctuaries. The interest of ancient constructors in these zones is also confirmed by data about inclinations, because of the great level of verticality of walls that was described in these zones. Finally, the great skills of the constructors in stages such as the staking out and excavation are also confirmed with data about orientations. The orientations of some aligned spaces show low deviations with respect to the straight line. In addition, we have found a clear orientation of QH33 with respect to the sunrise on the winter solstice. This supposes great skills both in planning, because this tomb avoided the intersection with QH32 (separated less than 10 cm in two zones), and astronomical knowledge.

Future work will include the analysis of parallelism and perpendicularity of elements based on geometries fitted to point clouds. We also want to apply this methodology to other great structures of the Necropolis in order to determine similarities and information about the evolution of these constructions. In addition, we want to develop other geometric studies of these tombs, mainly the funerary zones. We are sure that these structures still have several secrets to reveal about the construction skills of ancient Egyptians.

References

Ahmon, J. (2004). The application of short-range 3D laser scanning for archaeological replica production: the Egyptian tomb of Seti I. *The Photogrammetric Record*, *19*(106), 111-127. https://doi.org/10.1111/j.1477-9730.2004.00034.x

Alshawabkeh, Y., & Haala, N. (2004). Integration of digital photogrammetry and laser scanning for heritage documentation. *The International Archives of Photogrammetry and Remote Sensing*, *35*, B5.

Angelini, A., Vittozzi, G. C., & Baldi, M., (2016). The high official Harkhuf and the inscriptions of his tomb in Aswan (Egypt). An integrated methodological approach. *Acta IMEKO*, *5*(2), 71-79. http://doi.org/10.21014/acta_imeko.v5i2.349

Barazzetti, L., Previtali, M., & Roncoroni, F. (2017a). 3D Modelling with the Samsung Gear 360. *The International Archives of the Photogrammetry, Remote Sensing and Spatial Information Sciences*, *XLII-2-W3*, 85-90. https://doi.org/10.5194/isprs-archives-XLII-2-W3-85-2017

Barazzetti, L., Previtali, M., & Roncoroni, F. (2017b). Fisheye lenses for 3D modeling: evaluations and considerations. *The International Archives of the Photogrammetry, Remote Sensing and Spatial Information Sciences*, *XLII-2/W3*, 79-84. https://doi.org/10.5194/isprs-archives-XLII-2-W3-79-2017

Barazzetti, L., Previtali, M., & Roncoroni, F. (2022) 3D modeling with 5K 360° videos. *The International Archives of the Photogrammetry, Remote Sensing and Spatial Information Sciences*, *XLVI-2/W1-2022*, 65-71, https://doi.org/10.5194/isprs-archives-XLVI-2-W1-2022-65-2022

Beraldin, J. A., Blais, F., Boulanger, P., Cournoyer, L., Domey, J., El-Hakim, S. F., Godin, G., Rioux, M., & Taylor, J. (2000). Real world modelling through high resolution digital 3D imaging of objects and structures. *ISPRS Journal of Photogrammetry and Remote Sensing*, *55*(4), 230-250. https://doi.org/10.1016/S0924-2716(00)00013-7

Blockley, P., & Morandi, S. (2015). The recording of two late Roman towers, Archaeological Museum, Milan 3D documentation and study using image-based modelling. In *Digital Heritage 2015,* IEEE (pp. 103-106). Granada, Spain.

Brutto, M. L., & Meli, P. (2012). Computer vision tools for 3D modelling in archaeology. *International Journal of Heritage in the Digital Era*, *1*, 1-6. https://doi.org/10.1260/2047-4970.1.0.1

Campana, S. (2017). Drones in Archaeology. State-of-the-art and Future Perspectives. *Archaeological Prospection*, *24*(4), 275-296. https://doi.org/10.1002/arp.1569

Cardenal, J., Mata, E., Castro, P., Delgado, J., Hernandez, M. A., Pérez, J. L., Ramos, M., & Torres, M. (2004). Evaluation of a digital non metric camera (Canon D30) for the photogrammetric recording of historical buildings. *The International Archives of the Photogrammetry, Remote Sensing and Spatial Information Sciences*, *XXXV-B5*, 564-569.

Celikoyan, T. M., Altan, M. O., Kemper, G., & Toz, G. (2003). Calibrating and using an Olympus camera for balloon photogrammetry. In *Proc. XIXth International Symposium-CIPA 2003* (pp. 380-382). Antalya, Turkey.

Chandler, J. H., Fryer, J. G., & Jack, A. (2005). Metric capabilities of low-cost digital cameras for close range surface measurement. *The Photogrammetric Record*, *20*(109), 12-26. https://doi.org/10.1111/j.1477-9730.2005.00302.x

CIPA Heritage Documentation (2017). The photogrammetric capture. The '3x3' rules. Retrieved October 17, 2022, from https://www.cipaheritagedocumentation.org/

Colomina, I., & Molina, P. (2014). Unmanned aerial systems for photogrammetry and remote sensing: A review. *ISPRS Journal of Photogrammetry and Remote Sensing*, *92*, 79-97. https://doi.org/10.1016/j.isprsjprs.2014.02.013

Colonnese, F., Carpiceci, M., & Inglese, C. (2016). Conveying Cappadocia. A new representation model for rock-cave architecture by contour lines and chromatic codes. *Virtual Archaeology Review*, *7*(14), 13-19. https://doi.org/10.4995/var.2016.5382

Covas, J., Ferreira, V., & Mateus, L., (2015). 3D reconstruction with fisheye images strategies to survey complex heritage buildings. In *Digital Heritage 2015,* IEEE (pp. 123-126). Granada, Spain.

Echeverría, E., Celis, F., Morales, A., & da Casa, F. (2019). The Tomb of Ipi: 3D Documentation in a Middle Kingdom Theban Necropolis (Egypt, 2000 BCE). *The International Archives of the Photogrammetry, Remote Sensing and Spatial Information Sciences*, *XLII-2/W9*, 319-324. https://doi.org/10.5194/isprs-archives-XLII-2-W9-319-2019

Edel, E. (2008). Die Felsgräbernekropole der Qubbet el Hawa bei Assuan: I. Abteilung (Band 1-3). Architektur, Darstellungen, Texte, archäologischer Befund und Funde der Gräber QH 24-QH 209. In K. J. Seyfried & G. Vieler (Eds.), *Die Felsgräbernekropole der Qubbet el Hawa bei Assuan*. Paderborn, Germany: Ferdinand Schöningh.

Farella, E. M. (2016). 3D mapping of underground environments with a hand-held laser scanner. *Bollettino della società italiana di fotogrammetria e topografia*, *2*, 1-10.

Fiorillo, F., Limongiello, M., & Fernández-Palacios, B. J. (2016). Testing GoPro for 3D model reconstruction in narrow spaces. *Acta IMEKO*, *5*(2), 64-70. http://dx.doi.org/10.21014/acta_imeko.v5i2.372

Furukawa, Y., & Hernández, C. (2015). Multi-view stereo: A tutorial. *Foundations and Trends® in Computer Graphics and Vision*, *9*(1-2), 1-148. https://doi.org/10.1561/0600000052

Gardón-Ramos, V. (2021). The Geometrical Pattern in the Royal Architecture of Ancient Egypt during the Middle Kingdom. *Historiae*, (18), 45-70.

Georgopoulos, A., Karras, G. E., & Makris, G. N. (2003). The photogrammetric survey of a prehistoric site undergoing removal. *The Photogrammetric Record*, *16*(93), 443-456. https://doi.org/10.1111/0031-868X.00135

Grussenmeyer, P., Landes, T., Voegtle, T., & Ringle, K. (2008). Comparison methods of terrestrial laser scanning, photogrammetry and tacheometry data for recording of cultural heritage buildings. *The International Archives of the Photogrammetry, Remote Sensing and Spatial Information Sciences*, XXXVII/B5, 213–218.

Guarnieri, A., Remondino, F., & Vettore, A. (2006). Digital photogrammetry and TLS data fusion applied to Cultural Heritage 3D modeling. *The International Archives of the Photogrammetry, Remote Sensing and Spatial Information Sciences*, *36* (Part 5).

Harrell, J. A. (2008). Tools used in ancient Egyptian construction. *Encyclopedia of the History of Science, Technology, and Medicine in Non-Western Cultures (2nd ed.)*, (pp. 2158-2166). Dordrecht: Springer.

Hassani, F., Moser, M., Rampold, R., & Wu, C. (2015). Documentation of cultural heritage; techniques, potentials, and constraints. *The International Archives of the Photogrammetry, Remote Sensing and Spatial Information Sciences*, *40*(5), 207. https://doi.org/10.5194/isprsarchives-XL-5-W7-207-2015

Joyanes-Diaz, M., Martinez-De Dios, J., Mozas-Calvache, A., Ruiz-Jaramillo, J., Muñoz-Gonzalez, C., & Jimenez-Serrano, A. (2022). Solar geometry and the organization of the annual cycle through architecture and the funerary landscape in Qubbet el Hawa. *Mediterranean Archaeology and Archaeometry*, *22*(2), 209-235. https://www.doi.org/10.5281/zenodo.6815469

Kadobayashi, R., Kochi, N., Otani, H., & Furukawa, R. (2004). Comparison and evaluation of laser scanning and photogrammetry and their combined use for digital recording of cultural heritage. *The International Archives of the Photogrammetry, Remote Sensing and Spatial Information Sciences*, *35*(5), 401-406.

Koenderink, J. J., & Van Doorn, A. J. (1991). Affine structure from motion. *Journal of the Optical Society of America A*, *8*(2), 377-385.

Lambers, K., & Remondino, F. (2007). Optical 3D measurement techniques in archaeology: recent developments and applications. In *Proc. of the 35th International Conference on Computer Applications and Quantitative Methods in Archaeology* (pp. 27-35). Berlin, Germany.

Lima de, R., & Vergauwen, M. (2018). From TLS recoding to VR environment for documentation of the Governor's Tombs in Dayr al-Barsha, Egypt. In *2018 IEEE International Symposium on Mixed and Augmented Reality Adjunct (ISMAR-Adjunct)* (pp. 293-298). Munich, Germany.

Lowe, D. G. (2004). Distinctive image features from scale-invariant keypoints. *International Journal of Computer Vision*, *60*(2), 91-110. https://doi.org/10.1023/B:VISI.0000029664.99615.94

Mandelli, A., Gobeil, C., Greco, C., & Rossi, C. (2021). Digital twin and 3d documentation of a Theban tomb at Deir Al-Medina (Egypt) using a multi-lenses photogrammetric approach. *The International Archives of the Photogrammetry, Remote Sensing and Spatial Information Sciences*, *XLIII-B2-2021*, 591-597. https://doi.org/10.5194/isprs-archives-XLIII-B2-2021-591-2021

Martínez, S., Ortiz, J., Gil, M. L., & Rego, M. T. (2013). Recording complex structures using close range photogrammetry: The cathedral of Santiago de Compostela. *The Photogrammetric Record*, *28*(144), 375-395. https://doi.org/10.1111/phor.12040

Martínez Hermoso, J. A., Martínez Hermoso, F., de Paula Montes Tubío, F., & Jiménez Serrano, A. (2015). Geometry and proportions in the funeral chapel of Sarenput II. *Nexus Network Journal*, *17*(1), 287-309. https://doi.org/10.1007/s00004-014-0218-4

Martínez-Hermoso, J. A., Mellado-García, I., Martínez de Dios, J. L., Martínez-Hermoso, F., Espejo-Jiménez, A., & Jiménez-Serrano, A. (2018). The construction of tomb group QH31 (Sarenput II) through QH33. Part I: The exterior of the funerary complexes. *The Journal of Ancient Egyptian Architecture*, *3*, 25-44.

Mozas-Calvache, A. T., Pérez-García, J. L., Cardernal-Escarcena, F. J., Delgado, J., & Mata de Castro, E. (2012). Comparison of Low Altitude Photogrammetric Methods for Obtaining Dems and Orthoimages of Archaeological Sites. *The International Archives of the Photogrammetry, Remote Sensing and Spatial Information Sciences*, *XXXIX-B5*, 577-581. https://doi.org/10.5194/isprsarchives-XXXIX-B5-577-2012

Mozas-Calvache, A. T., Pérez-García, J. L., Gómez-López, J. M., de Dios, J. M., & Jiménez-Serrano, A. (2020). 3D models of the QH31, QH32 and QH33 tombs in Qubbet el Hawa (Aswan, Egypt). *The International Archives of the Photogrammetry, Remote Sensing and Spatial Information Sciences*, *XLIII-B2-2020*, 1427-1434. https://doi.org/10.5194/isprs-archives-XLIII-B2-2020-1427-2020

Nabil, M., Betrò, M., & Metwallya, M. N. (2013). 3D reconstruction of ancient Egyptian rockcut tombs: the case of Midan 05. *The International Archives of the Photogrammetry, Remote Sensing and Spatial Information Sciences*, *XL-5/W2*, 443-447. https://doi.org/10.5194/isprsarchives-XL-5-W2-443-2013

Nex, F., & Remondino, F. (2014). UAV for 3D mapping applications: a review. *Applied Geomatics*, *6*(1), 1-15. https://doi.org/10.1007/s12518-013-0120-x

Ogleby, C. L., Papadaki, H., Robson, S., & Shortis, M. R. (1999). Comparative camera calibrations of some "off the shelf" digital cameras suited to archaeological purposes. *The International Archives of the Photogrammetry, Remote Sensing and Spatial Information Sciences*, *XXXII-5/W11*, 69-75.

Ortiz, J., Gil, M. L., Martínez, S., Rego, T., & Meijide, G. (2013). Three-dimensional Modelling of Archaeological Sites Using Close-range Automatic Correlation Photogrammetry and Low-altitude Imagery. *Archaeological Prospection*, *20*(3), 205-217. https://doi.org/10.1002/arp.1457

Pérez-García, J. L., Mozas-Calvache, A. T., Gómez-López, J. M., & Jiménez-Serrano, A. (2018). Three-dimensional modelling of large archaeological sites using images obtained from masts. Application to Qubbet el-Hawa site (Aswan, Egypt). *Archaeological Prospection*, *26*(2), 121-135. https://doi.org/10.1002/arp.1728

Pérez-García, J. L., Mozas-Calvache, A. T., Barba-Colmenero, V., & Jiménez-Serrano, A. (2019). Photogrammetric studies of inaccessible sites in archaeology: Case study of burial chambers in Qubbet el-Hawa (Aswan, Egypt). *Journal of Archaeological Science*, 102, 1-10. https://doi.org/10.1016/j.jas.2018.12.008

Perfetti, L., Polari, C., & Fassi, F. (2017). Fisheye Photogrammetry: Tests and Methodologies for the Survey of Narrow Spaces. *International Archives of Photogrammetry and Remote Sensing*, *XLII-2/W3*, 573-580. https://doi.org/10.5194/isprs-archives-XLII-2-W3-573-2017

Perfetti, L., & Fassi, F. (2022). Handheld fisheye multicamera system: surveying meandering architectonic spaces in open-loop mode – accuracy assessment. *The International Archives of the Photogrammetry, Remote Sensing and Spatial Information Sciences*, *XLVI-2/W1-2022*, 435-442. https://doi.org/10.5194/isprs-archives-XLVI-2-W1-2022-435-2022

Remondino, F., Rizzi, A., Jimenez, B., Agugiaro, G., Baratti, G., & De Amicis, R. (2011). The Etruscans in 3D: From space to underground. *Geoinformatics*, *6*, 283-290. https://doi.org/10.14311/gi.6.35

Rossi, C. (2001). Dimensions and slope in the nineteenth and twentieth dynasty royal tombs. *The Journal of Egyptian Archaeology*, *87*(1), 73-80. https://doi.org/10.1177/030751330108700107

Sánchez-León, J. C., & Jiménez-Serrano, A. (2015). Sattjeni: Daughter, Wife and Mother of the Governors of Elephantine during the End of the Twelfth Dynasty. *Zeitschrift für Ägyptische Sprache und Altertumskunde*, *142*(2), 154-166. https://doi.org/10.1515/zaes-2015-0013

Sánchez-León, J. C., & Jiménez-Serrano, A. (2016). Keeping provincial power in the lineage during the Twelfth Dynasty: The case of Khema, governor of Elephantine. *Studien zur Altägyptischen Kultur*, 307-314.

Scharstein, D., & Szeliski, R. (2002). A taxonomy and evaluation of dense two-frame stereo correspondence algorithms. *International Journal of Computer Vision*, *47*(1-3), 7-42. https://doi.org/10.1109/SMBV.2001.988771

Seitz, S. M., Curless, B., Diebel, J., Scharstein, D., & Szeliski, R. (2006). A comparison and evaluation of multi-view stereo reconstruction algorithms. In *IEEE Computer Society Conference on Computer Vision and Pattern Recognition* (pp. 519-528). New York, USA.

Shaltout, M., & Belmonte, J. A. (2005). On the orientation of ancient Egyptian temples: (1) Upper Egypt and Lower Nubia. *Journal for the History of Astronomy*, *36*(3), 273-298. https://doi.org/10.1177/002182860503600302

Szeliski, R. (2011). *Computer Vision: Algorithms and Applications*. London: Springer.

Ullman, S. (1979). The interpretation of structure from motion. *Proceedings of the Royal Society of London B*, *203*, 405-426. https://doi.org/10.1098/rspb.1979.0006

Waldhäusl, P., & Ogleby, C. L. (1994). 3 x 3 rules for simple photogrammetric documentation of architecture. *The International Archives of Photogrammetry and Remote Sensing*, *30-5*, 426-429.

Westoby, M. J., Brasington, J., Glasser, N. F., Hambrey, M. J., & Reynolds, J. M. (2012). 'Structure-from-Motion' photogrammetry: A low-cost, effective tool for geoscience applications. *Geomorphology*, *179*, 300-314. https://doi.org/10.1016/j.geomorph.2012.08.021

Zlot, R., & Bosse, M. (2014). Three-dimensional mobile mapping of caves. *Journal of Cave & Karst Studies*, *76(3)*, 191-206. https://doi.org/10.4311/2012EX0287